arXiv:1407.4168v1 [astro-ph.CO] 15 Jul 2014

THE EXTENDED ZEL'DOVICH MASS FUNCTIONS OF CLUSTERS AND ISOLATED CLUSTERS IN THE PRESENCE OF PRIMORDIAL NON-GAUSSIANITY

Seunghwan Lim[1], Jounghun Lee[2]

ABSTRACT

We present new formulae for the mass functions of the clusters and the isolated clusters with non Gaussian initial conditions. For this study, we adopt the Extended Zel'dovich (EZL) model as a basic framework, focusing on the case of primordial non-Gaussianity of the local type whose degree is quantified by a single parameter f_{nl}. By making a quantitative comparison with the N-body results, we first demonstrate that the EZL formula with the constant values of three fitting parameters still works remarkably well for the local f_{nl} case. We also modify the EZL formula to find an analytic expression for the mass function of isolated clusters which turns out to have only one fitting parameter other than the overall normalization factor and showed that the modified EZL formula with a constant value of the fitting parameter matches excellently the N-body results with various values of f_{nl} at various redshifts. Given the simplicity of the generalized EZL formulae and their good agreements with the numerical results, we finally conclude that the EZL mass functions of the massive clusters and isolated clusters should be useful as an analytic guideline to constrain the scale dependence of the primordial non-Gaussianity of the local type.

Subject headings: cosmology:theory — large scale structure of universe

1. INTRODUCTION

The three pillars which have founded and sustained the concordance cosmology are the Cosmic Microwave Background (CMB) spectrum, the luminosity-distance relation of the

[1]Department of Astronomy, University of Massachusetts, LGRT-B 619E, 710 North Pleasant Street, Amherst, MA 01003-9305, USA; slim@astro.umass.edu

[2]Astronomy Program, Department of Physics and Astronomy, FPRD, Seoul National University, Seoul 151-747, Korea; jounghun@astro.snu.ac.kr

type Ia Supernovae (SNIa), and the statistics of the large-scale structures. The sensational concord among the three observables depicts a simple universe whose initial conditions are exhaustively specified by the following six key cosmological parameters: the matter density parameter (Ω_m), the cosmological constant Λ parameter (Ω_Λ), the baryon density parameter (Ω_b), the dimensionless Hubble parameter (h), the amplitude of the linear density power spectrum (σ_8), and the spectral index (n_s) (for a recent review, see Hamilton 2013).

The recently reported tensions among the three on the best-fit values of the key parameters, however, have implied that the concordance cosmology might be a misnomer. For instance, the Planck CMB analysis yielded the value of h to be 0.673 ± 0.012 (Planck Collaboration XVI. 2013), which differs substantially from the value, $h = 0.738 \pm 0.024$, determined by the HST (Hubble Space Telescope) observation of the SNIa (Riess et al. 2011). A more significant tension with the CMB result was found in the locally determined best-fit value of σ_8: The redshift evolution of the SZ (Sunyaev-Zel'dovich) cluster counts traced by the Planck team found $\sigma_8 = 0.77 \pm 0.02$ (Planck Collaboration XX. 2013) while the best-fit value from the Planck CMB data was $\sigma_8 = 0.834 \pm 0.027$ (Planck Collaboration XVI. 2013).

Although our confidence in the concordance cosmology has yet to be shattered down, these discrepancies definitely required us not only to search for possible systematics in observational data analysis but also to carefully reexamine whether or not our theoretical modeling of the three observables is accurate enough to predict the initial conditions of the universe. Especially, the statistical properties of the large scale structures are hard to model accurately by using only the first principles since the formation and evolution of the large scale structures occurred in the complicated nonlinear regime (e.g., see Springel et al. 2006).

The cluster mass function is defined as the number density of the galaxy clusters per mass bin per unit volume. It exhibits exponential dependence on the cluster mass, corresponding to the high-mass section of the halo mass function. It is one of those few statistics of the large-scale structures which have a direct connection with the initial conditions of the universe. When Press & Schechter (1974) proposed for the first time an analytic prescription of deriving the halo mass function from the initial Gaussian density field, their work could not attract much attention mainly due to its statistical flaw. However, ever since Bond et al. (1991) refined and improved the Press-Schechter formalism with the help of the celebrated excursion set theory, the halo mass function has been the subject of the extensive analytic studies (e.g., Jedamzik 1995; Monaco 1995; Bond & Myers 1996a,b; Yano et al. 1996; Audit et al. 1997; Monaco 1997a,b; Lee & Shandarin 1998; Sheth et al. 2001; Chiueh & Lee 2001; Sheth & Tormen 2002; Shen et al. 2006; Desjacques 2008; Maggiore & Riotto 2010a,b; Corasaniti & Achitouv 2011a,b; Musso & Sheth 2012; Paranjape et al. 2012; Paranjape & Sheth 2012; Achitouv & Corasaniti 2012; Paranjape et al. 2013; Achitouv et al. 2013a,b).

While the above analytic studies have indeed enlightened us about how to relate the number densities of dark halos to the statistical properties of the linear density field and how to account for the effect of environments on the halo mass function, it has been gradually realized that the level of the accuracy required for the cluster mass function to be useful as a probe of precision cosmology can be achieved only by adjusting the analytic mass functions to the numerical results from N-body simulations. The advent of high-resolution N-body simulations and the necessity of having a practical but accurate mass function led many authors to come up with empirical formulae, most of which have pulled it off to match the numerical results within 20% errors at the expense of giving up physical understanding (e.g., Sheth & Tormen 1999; Jenkins et al. 2001; Warren et al. 2006; Tinker et al. 2008; Crocce et al. 2010; Pillepich et al. 2010; Courtin et al. 2011).

The extended Zel'dovich (EZL) formula recently proposed by Lim & Lee (2013) is one of those empirical formulae which showed remarkable agreements with various N-body results when their fitting parameters are numerically adjusted. Unlike the other formulae, however, the EZL mass function has a good advantage that the empirically determined best-fit values of their three characteristic parameters are constant at various redshifts even when the key cosmological parameters of the standard ΛCDM model change. Given this advantage, Lim & Lee (2013) speculated that the EZL mass function of galaxy clusters would provide a tight constraint on the dark energy equation of state provided that it is valid even for non-standard cosmologies. Very recently, Lim & Lee (2014) showed that a modified version of the EZL formula is very useful to analytically evaluate the mass function of the superclusters.

As a first step toward testing the validity of the EZL model for non-standard cosmologies, we will investigate here whether or not it works even in the presence of primordial non-Gaussianity. As it has been well known, primordial non-Gaussianity is one of the hottest issues in the field of inflation since detection of a significant signal of primordial non-Gaussianity would rule out the single field slow-roll inflation model (for a review, see Bartolo et al. 2004). Although the degree of primordial non-Gaussianitiy on the CMB scale has been found to be almost undetectably small (Planck Collaboration XXIV. 2013), the Planck results have yet to demolish the mission to search for a signal of primordial non-Gaussianity on the cluster-mass scale given that primordial non-Gaussianity could be scale-dependent.

Plenty of literatures have already studied the effect of primordial non-Gaussianity on the cluster abundance and its evolution (e.g., Lucchin & Matarrese 1988; Matarrese et al. 2000; Verde et al. 2001; Benson et al. 2002; Scoccimarro et al. 2004; Lo Verde et al. 2008; Dalal et al. 2008; Lam & Sheth 2009b; Lam et al. 2009; Maggiore & Riotto 2010c; Pillepich et al. 2010; de Simone et al. 2011; Achitouv & Corasaniti 2012). The most optimal formula for the

cluster mass function as a probe of primordial non-Gaussianity, however, should be the one which exhibit not only excellent agreements with the numerical results but also insensitivity of its fitting parameters to the redshifts, background cosmology and the presence of primordial non-Gaussianity. In this Paper, we will also modify the EZL formula to find an accurate formula for the mass function of the isolated clusters which is expected to be more sensitive to the presence of primordial non-Gaussianity (Song & Lee 2009; Lee 2012; Achitouv & Corasaniti 2012) and examine its limitation as well as usefulness as a probe of primordial non-Gaussianity.

2. THE EZL MASS FUNCTION OF ALL CLUSTERS

2.1. The Original Formula : A Brief Review

The halo mass function, $dN(M,z)/d\ln M$, represents the differential number density of the bound halos in a logarithmic mass interval of $[\ln M,\ \ln M + d\ln M]$ at redshift z per unit volume. It depends sensitively on the background cosmology via its dependence on the rms fluctuation of the linear density field on the mass scale M at redshift z, $\sigma(M,z) \equiv D(z)\sigma(M,0)$ where $D(z)$ is the linear growth factor that has a value of unity at the present epoch (for a recent review, see Zentner 2007).

The extended Zel'dovich (EZL) model is an empirical formula for the halo mass function characterized by three fitting parameters, recently developed by Lim & Lee (2013), under the usual assumption that the primordial density field is Gaussian random:

$$\int_C \Pi_{i=1}^3 d\lambda_i\, p[\vec{\lambda};\sigma(M,z)] = \int_{\ln M}^{\infty} d\ln M' \frac{M'}{\bar{\rho}} \frac{dN(M',z)}{d\ln M'} P(\vec{\lambda} \geq \vec{\lambda}_c | \vec{\lambda}' = \vec{\lambda}_c)\,, \qquad (1)$$

where three eigenvalues (in a decreasing order) of the linear deformation tensor on the mass scale of M and M' are denoted as $\vec{\lambda} \equiv (\lambda_1, \lambda_2, \lambda_3)$ and $\vec{\lambda}' \equiv (\lambda_1', \lambda_2', \lambda_3')$, respectively.

As mentioned in Lim & Lee (2013), the EZL model was established in the framework of the Jedamzik formalism (Jedamzik 1995). In the right hand side of Equation (1), $(M'/\rho)dN/d\ln M'$ (with mean mass density ρ) represents the differential fraction of the volume of the linear density field occupied by the proto-halo regions where three eigenvalues reach the thresholds as $\vec{\lambda}_c \equiv (\lambda_{1c}, \lambda_{2c}, \lambda_{3c})$ when the linear density field is smoothed on the mass scale of M', and $P(\vec{\lambda} \geq \vec{\lambda}_c | \vec{\lambda}' = \vec{\lambda}_c)$ represents the conditional probability of finding a region embedded in the proto-halos regions where the three eigenvalues exceed the thresholds on some lower mass scale $M \leq M'$.

Integration of the differential volume fraction multiplied by the conditional mass func-

tion over $\ln M'$ in the right-hand side of Equation (1) excludes the contributions from the clouds-in-clouds to the cumulative probability that the linear shear eigenvalues $\vec{\lambda}$ exceed the given thresholds $\vec{\lambda}_c$ on the mass scale of M expressed in the left-hand side of Equation (1):

$$\int_C \Pi_{i=1}^3 d\lambda_i \, p[\vec{\lambda}; \sigma(M)] = \int_{\lambda_{1c}}^{\infty} d\lambda_1 \int_{\lambda_{2c}}^{\lambda_1} d\lambda_2 \int_{\lambda_{3c}}^{\lambda_2} d\lambda_3 \, p[\vec{\lambda}; \sigma(M)] \,, \tag{2}$$

where $p(\lambda_1, \lambda_2, \lambda_3)$ is the joint probability density distribution of the linear shear eigenvalues, which was first derived in the seminal paper of Doroshkevich (1970). The conditional probability, $P(\vec{\lambda} \geq \vec{\lambda}_c | \vec{\lambda}' = \vec{\lambda}_c)$, in the right-hand side of Equation (1) can be calculated as

$$\frac{\int_{\lambda_{1c}}^{\infty} d\lambda_1 \int_{\lambda_{2c}}^{\lambda_1} d\lambda_2 \int_{\lambda_{3c}}^{\lambda_2} d\lambda_3 \; p(\lambda_1, \lambda_2, \lambda_3, \lambda_1' = \lambda_{1c}, \lambda_2' = \lambda_{2c}, \lambda_3' = \lambda_{3c})}{p(\lambda_1' = \lambda_{1c}, \lambda_2' = \lambda_{2c}, \lambda_3' = \lambda_{3c})} \,. \tag{3}$$

The analytic expression for the joint probability density distribution, $p(\vec{\lambda}, \vec{\lambda}')$, in Equation (3) has been found in Desjacques (2008) and Desjacques & Smith (2008).

Similar to the original formula of Jedamzik (1995), the EZL formula is an integro-differential equation which yields an automatically normalized mass function. Unlike the original Jedamzik formula, however, it is not a physical model but a mere empirical formula whose three characteristic parameters, $\vec{\lambda}_c$, have to be determined empirically via fitting and thus the best-fit values of $\vec{\lambda}_c$ have nothing to do with a real physical condition for the gravitational collapse. Nevertheless, the best-fit values of the EZL parameters were found by Lim & Lee (2013) to be constant against the variation of redshifts and the initial conditions.

2.2. Incorporation of the non-Gaussian Initial Conditions

In the current work we focus on the case of primordial non-Gaussianity of the local type where the deviation of the primordial velocity potential field (Φ) from an Gaussian random field (ϕ) is approximated at first oder as $\Phi \approx \phi + f_{nl}(\phi^2 - \langle \phi^2 \rangle)$ where f_{nl} is called the (local) primordial non-Gaussianity parameter (see, Babich et al. 2004; Lo Verde et al. 2008). Lam et al. (2009) showed that in the presence of primordial non-Gaussianity of the local type the probability density distribution of the shear eigenvalues, $p_{\rm ng}(\vec{\lambda}; \sigma)$, is approximated at first order as

$$p_{\rm ng}(\vec{\lambda}; \sigma) \approx \Big[1 + \frac{\sigma S_3}{6} H_3\Big(\frac{\delta}{\sigma}\Big)\Big] p(\vec{\lambda}; \sigma) \,, \tag{4}$$

where the H_3 is the third order Hermite polynomial given as $H_3(x) = x(x^2 - 3)$ and $p(\vec{\lambda}; \sigma)$ and is the probability density distribution of the shear eigenvalues for the Gaussian case ($f_{nl} = 0$).

The skewness parameter, S_3, in Equation (4), is related to f_{nl}, as (Lo Verde et al. 2008; Lam et al. 2009)

$$\sigma S_3 \equiv \frac{\langle \delta^3 \rangle}{\langle \delta^2 \rangle^{3/2}} = \frac{2 f_{nl} \gamma^3}{\sigma^3} \,. \tag{5}$$

Here σ and γ are given as

$$\sigma^2 = \frac{1}{(2\pi)^3} \int \frac{dk}{k} 4\pi k^7 M^2(k) P_\Phi(k) W^2(kR), \tag{6}$$

$$\gamma^3 = \frac{2}{(2\pi)^4} \int \frac{dk_1}{k_1} k_1^5 M(k_1) W(k_1 R) \int \frac{dk_2}{k_2} k_2^5 M(k_2) W(k_2 R) \times \int d\mu_{12} k_{12}^2 M(k_{12}) W(k_{12} R) \frac{B_\Phi(k_1, k_2, k_{12})}{2 f_{nl}} \tag{7}$$

where $M(k) \equiv [3D(z)c^2 T(k)]/(5\Omega_m H_0^2)$ and $T(k)$ is the transfer function. The power spectrum, P_Φ, and the bispectrum, B_Φ, are approximated at first order as

$$P_\Phi(k) = P_\phi(k) + \mathcal{O}(f_{nl}^2) \,, \tag{8}$$

$$B_\Phi(k_1, k_2, k_{12}) = 2 f_{nl} [P_\phi(k_1) P_\phi(k_2) + \text{cyclic}] + \mathcal{O}(f_{nl}^3) \,, \tag{9}$$

In practice, we compute the skewness parameter, S_3, by employing the following approximate formula given in Achitouv & Corasaniti (2012):

$$S_3 = f_{nl} \frac{1.56}{\sigma^{0.84}} 10^{-4} \,. \tag{10}$$

With the help of the same perturbative technique that Lam et al. (2009) employed to derive Equation (4), one can straightforwardly show that the conditional probability density in the presence of primordial non-Gaussianity of the local type, $p_{\rm ng}(\vec{\lambda}|\vec{\lambda}' = \vec{\lambda}_c)$, can be approximated at first order as

$$p_{\rm ng}(\vec{\lambda}|\vec{\lambda}' = \vec{\lambda}_c) = \left[1 + \frac{\sigma S_3}{6} H_3\Big(\frac{\delta}{\sigma}\Big) \right] p(\vec{\lambda}|\vec{\lambda}' = \vec{\lambda}_c) \,. \tag{11}$$

Replacing $p(\vec{\lambda})$ in Equation (2) by $p_{\rm ng}(\vec{\lambda})$ in Equation (4) and $p(\vec{\lambda}|\vec{\lambda}' = \vec{\lambda}_c)$ in Equation (3) by $p_{\rm ng}(\vec{\lambda}|\vec{\lambda}' = \vec{\lambda}_c)$ in Equation (11), one can compute the EZL mass function of dark halos in the presence of primordial non-Gaussianity of the local-type.

It is worth explaining here why we restrict our analysis to the local f_{nl} case. When Lam et al. (2009) derived Equation (4), it was assumed that the only non-vanishing skewness is the linear density contrast $\delta \equiv \sum_{i=1}^{3} \lambda_i$. This key assumption is valid only for the case of primordial non-Gaussianity of the local type which does not modify the shape of the

probability density distribution of the shear eigenvalues (private communication with T.Y. Lam 2014). For the other types which depend explicitly on the shape it is expected that the joint probability density of the shear eigenvalues will be different from Equation (4), the derivation of which is beyond the scope of this paper.

2.3. Comparison with N-body Results

To numerically test the EZL mass functions for the local f_{nl} case, we make a use of the samples of dark matter halos from a large N-body simulation provided by C. Wagner through private communication. While the detailed full description of the N-body simulation can be found in Wagner et al. (2010) and Wagner & Verde (2012), let us provide relevant key information on the numerical data used for the current work: Wagner et al. (2010) utilized the publicly available gadget-2 code (Springel 2005) to run a N-body simulation of 1024^3 dark matter particles in a periodic box of linear size $L_{\rm box} = 1875\,h^{-1}$Mpc for a flat ΛCDM model with non-Gaussian initial conditions with the key cosmological parameters set at $\Omega_m = 0.27,\ \Omega_b = 0.047,\ h = 0.7,\ n_s = 0.95,\ \sigma_8 = 0.7913$. They have identified the dark halos with the Amiga's Halo Finder which calculates the halo mass by considering all particles inside a sphere within which a mean overdensity reaches some "redshift dependent" virial overdensity (Knollmann & Knebe 2009). From their simulations were produced the samples of the dark halos with mass $M \geq 10^{13}\,h^{-1}M_{\odot}$ at three different redshifts ($z = 0,\ 0.67,\ 1$) for two different cases of primordial non-Gaussianity of the local type ($f_{nl} = 60,\ 250$) as well as for the Gaussian case ($f_{nl} = 0$).

As done in Wagner et al. (2010), we determine the numerical mass function of dark halos at each redshift as the differential number density of the dark halos per logarithmic mass bins divided by the total volume of the simulation. To estimate the errors associated with the determination of the numerical mass function of the dark halos, the sample of the dark halos is divided into eight subsamples, each of which has the same size. For each subsample, the number counts are recalculated and then the Jackknife errors per each logarithmic mass bin is calculated as the standard deviation scatter among the eight subsamples.

When Lim & Lee (2013) fitted the EZL mass function to the numerical results to determine its best-fit parameters , the numerical results they used were obtained from dark halos identified by the conventional halo-finding algorithms such as the friends-of-friends (FoF) and the spherical over density (SO) algorithm. Whereas the dark halos from the N-body simulations of (Wagner et al. 2010) used in the current work were identified by the Amigo's Halo Finder that is different from the conventional halo finding scheme. Therefore, one might expect that the best-fit values of the model parameters of the EZL mass function could be

different from those found in the original work of (Lim & Lee 2013). Fitting the EZL model to the numerical mass function at $z = 0$ for the Gaussian case by adjusting the three model parameters, we determine the best-fit values as $\lambda_{1c} = 0.56,\ \lambda_{2c} = 0.555,\ \lambda_{3c} = 0.32$, which turn out to be identical to the best-fit values found by (Lim & Lee 2013) for the case of the SO halos, indicating the robustness of the EZL formula.

The top panels of Figure 1 show the numerical mass functions (dots) with the Jackknife errors as well as the EZL mass functions at three different redshifts ($z = 0, 0.67$ and 1 as the solid, dotted and dashed lines, respectively) for three different cases of the local non-Gaussianity ($f_{nl} = 0,\ 60$ and 250 in the left, middle and right panel, respectively). The same values of the cosmological parameters that were used for the N-body simulations are implemented into the EZL formula, and the same values of the EZL model parameters as determined for the Gaussian case, $\lambda_1 = 0.56$, $\lambda_2 = 0.555$ and $\lambda_3 = 0.32$, are also implemented into the formula for three different cases of f_{nl}. As can be seen, for all of the three cases of f_{nl}, the constant values of the model parameters of the EZL formula yield excellent agreements with the numerical results at all redshifts, indicating that the EZL formula with the same parameters used for the Gaussian case still works very well even in the presence of primordial non-Gaussianity.

To quantify how good the agreements are, we also show the ratios of the EZL models to the numerical results in the bottom panel of Figure 1. In the mass-range of $M \leq 3 \times 10^{14}\, h^{-1} M_{\odot}$, the EZL model agrees with the numerical mass functions within 20% errors for all cases. In the higher mass section, however, the errors exceed 20%. The EZL formula exhibit better agreements with the numerical results at lower redshifts and for the case of small f_{nl}. The rather large deviation of the EZL formula from the numerical result for the case of $f_{nl} = 250$ should be due to the fact that the EZL mass function with the local-type non-Gaussianity was derived only at first order.

3. THE EZL MASS FUNCTION OF THE ISOLATED CLUSTERS

It is Song & Lee (2009) who have done the first feasibility study of using the abundance of the isolated clusters as a probe of primordial non-Gaussianity. Original as the idea of Song & Lee (2009) was, their analytic prescription of evaluating the mass function of the isolated clusters was such a crude approximation based on several oversimplified assumptions. In fact, their feasibility study was aimed only at presenting a proof of the concept that the mass function of the isolated clusters should be a more sensitive test of the presence of primordial non-Gaussianity than that of all clusters.

Lee (2012) constructed a much more accurate formula for the mass function of the isolated clusters for the Gaussian case in the framework of the "drifting barrier" (DB) formalism developed by Corasaniti & Achitouv (2011a,b). Achitouv & Corasaniti (2012) incorporated the effect of primordial non-Gaussianity into the DB model and confirmed that the abundance of the isolated clusters indeed varies more sensitively with the degree of primordial non-Gaussianity than that of all clusters. True as it is that the DB model of Achitouv & Corasaniti (2012) is capable of predicting quite accurately the abundance of the isolated clusters in the presence of primordial non-Gaussianity, the model parameters of the DB mass function were shown to be not constant against the changes of z and f_{nl} (Achitouv et al. 2013b).

Noting that the model parameters of the EZL mass function are found to have desirable independence on z and f_{nl} in section 2.3 and given that the dynamical process of the isolated clusters is expected to be much simpler than that of ordinary clusters located in over dense regions (Desjacques 2008), we now attempt to model the abundance of the isolated clusters for the local f_{nl} case by employing the following one dimensional (1D) EZL formula that has only one parameter other than the overall normalization factor (Lim & Lee 2013):

$$\int_{\lambda_{3c}}^{\infty} d\lambda_3\, p[\lambda_3; \sigma(M,z)] \propto \int_{\ln M}^{\infty} d\ln M' \frac{M'}{\bar{\rho}} \frac{dN_{\rm I}(M,z)}{d\ln M'} P(\lambda_3 \geq \lambda_{3c} | \lambda_3' = \lambda_{3c})\,, \qquad (12)$$

where $dN_{\rm I}/d\ln M$ denotes the mass function of the isolated clusters which have no neighbor clusters within a given threshold distance and A is the normalization factor whose value has to be determined empirically according to the constraint that the integration of the mass function of the isolated clusters must yield the total number of the isolated clusters in a given sample divided by the total volume (Lee 2012).

The left-hand side of Equation (12) represents the cumulative probability that the smallest shear eigenvalue , λ_3, is larger than the characteristic parameter, λ_{3c}, on the mass scale of M. The one-point probability density distribution of λ_3 can be obtained by integrating the three-point probability density of $\vec{\lambda}$ as (Lee & Shandarin 1998)

$$p(\lambda_3) = \int_{\lambda_3}^{\infty} d\lambda_1 \int_{\lambda_3}^{\lambda_1} d\lambda_2 p(\lambda_1, \lambda_2, \lambda_3)\,. \qquad (13)$$

The conditional probability, $P(\lambda_3 \geq \lambda_{3c} | \lambda_3' = \lambda_{3c})$, in the right-hand side of Equation (12) can be calculated as

$$P(\lambda_3 \geq \lambda_{3c} | \lambda_3' = \lambda_{3c}) = \frac{\int_{\lambda_{3c}}^{\infty} d\lambda_3\; p(\lambda_3, \lambda_3' = \lambda_{3c})}{p(\lambda_3' = \lambda_{3c})}\,, \qquad (14)$$

where $p(\lambda_3, \lambda_3')$ denotes the joint probability density distribution of the smallest eigenvalues on two different scales, M' and M, respectively, which can be obtained by integrating the

six-point probability density of $\vec{\lambda}$ and $\vec{\lambda}'$ as (Desjacques 2008):

$$p(\lambda_3, \lambda_3') = \int_{\lambda_3}^{\infty} d\lambda_1 \int_{\lambda_3}^{\lambda_1} d\lambda_2 \int_{\lambda_3'}^{\infty} d\lambda_1' \int_{\lambda_3'}^{\lambda_1'} d\lambda_2' \; p(\vec{\lambda}, \vec{\lambda}') \,. \tag{15}$$

To evaluate the mass function of the isolated clusters in the presence of primordial non-Gaussianity of the local type, we replace $p(\vec{\lambda})$ in Equation (13) by $p_{\rm ng}(\vec{\lambda})$ and $p(\vec{\lambda}, \vec{\lambda}')$ in Equation (15) by $p_{\rm ng}(\vec{\lambda}, \vec{\lambda}')$, respectively.

For the case of all clusters, it was shown by Lim & Lee (2013) that the 1D EZL formula characterized by only one parameter does not provide a good fit to the numerical results. However, for the case of the isolated clusters located in the under dense regions where the formation process is less affected by the environments, we speculate that the 1D EZL formula may work very well as the simpler formation process would be modeled by fewer parameters. To test this speculation against N-body simulations, we first construct a subsample of the isolated clusters from the N-body data described in section 2.3. Lee (2012) identified the isolated clusters as those which have no neighbor clusters within the distance of $0.4\bar{d}_c$ where $\bar{d}_c$ denotes the mean separation distance of the clusters in the sample. Basically, we apply the FoF algorithm with the linking length parameter of $b = 0.4$ to the cluster-size halos with mass larger than $10^{13}\, h^{-1} M_\odot$ in the cluster sample to find the FoF groups consisting of the clusters. Then, we select the isolated clusters as those FoF groups which have only one member cluster.

The total number and mean mass of the isolated clusters at $z = 0,\ 0.67$ and 1 are listed in Tables 1, 2 and 3, respectively. As one can see, there are more isolated clusters in the models with higher degree of primordial non-Gaussianity. Carrying out the same procedure as described in section 2.3, we count the number of the isolated clusters per logarithmic mass bin at each redshift for each case of the local f_{nl}. Then, we fit the 1D EZL formula at $z = 0$ for the case of $f_{nl} = 0$ to the numerical mass functions of the isolated clusters by adjusting the value of λ_{3c} in the 1D EZL formula, and find that $\lambda_{3c} = 0.5$ gives the best-fits. Then, plugging this same value of $\lambda_{3c} = 0.5$ into Equations (14), we examine whether the same value of λ_{3c} makes the 1D EZL formula for the case of non-zero value of f_{nl} match the numerical mass functions.

Figure 2 shows the same as Figure 1 but for the cases of the isolated clusters. For this plot, we renormalize the 1D EZL mass functions according to the condition of $\int dN_{\rm I}/d\ln M = N_{\rm I,tot}/V$, where $N_{\rm I,tot}$ represents the total number of the isolated clusters found in the sample at each redshift for each case of f_{nl} and V is the total volume of the simulation. As can be seen, the 1D EZL mass function with the constant value of its model parameter agrees with the numerical results within 20% errors in the mass range of $3{\times}10^{13} \leq M/(h^{-1}M_\odot) \leq 2{\times}10^{14}$ for every case.

To see how sensitively the mass function of the isolated clusters changes with the value of f_{nl}, we compute the ratio of $[dN_{\rm I}/d\ln M]_{f_{nl}\neq 0}$ to $[dN_{\rm I}/d\ln M]_{f_{nl}=0}$ where $[dN_{\rm I}/d\ln M]_{f_{nl}=0}$ and $[dN_{\rm I}/d\ln M]_{f_{nl}\neq 0}$ represent the mass functions of the isolated clusters for the Gaussian and the non-Gaussian case, respectively. Figure 3 plots this ratio in the right panel at $z = 0$, while the left panel shows the ratio of $[dN/d\ln M]_{f_{nl}\neq 0}$ to $[dN/d\ln M]_{f_{nl}=0}$ where $dN/d\ln M$ is the mass function of all clusters.

Note that the degree of the deviation of the ratio from unity is higher for the case of the isolated clusters than for the case of all clusters over the whole mass range. At the high mass end of $M \geq 2\cdot 10^{15}, h^{-1}M_{\odot}$, the number counts of the isolated clusters for the case of $f_{nl} = 250$ ($f_{nl} = 60$) exhibits $\sim 40\%$ ($\sim 10\%$) difference from those for the Gaussian case, while in the number counts of all clusters there is only $\sim 20\%$ ($\sim 5\%$) difference between the two cases. Figure 4 plots the same as Figure 3 but at $z = 1$, which reveals the same trend that the mass function of the isolated clusters in the high-mass end is twice more sensitive to the change of f_{nl}.

In practice the EZL mass function of the isolated clusters in the high-mass end would suffer inevitably from much larger Poisson errors than that of all clusters because the formation of massive clusters are strongly suppressed in the isolated under dense regions. In our analysis, it is found that the Poisson errors in the measurement of the number densities of the isolated clusters in the high-mass range of $10^{14} \leq M/(h^{-1}M_{\odot}) \leq 10^{15}$ are $(2-4)$ times larger than that of all clusters. But, Figure 3 also reveals that in the low-mass section $10^{13} \leq M/(h^{-1}M_{\odot}) \leq 10^{14}$ where the contamination by the Poisson errors is expected to be negligible, the ratio of $[dN_{\rm I}/d\ln M]_{f_{nl}=250}$ to $[dN_{\rm I}/d\ln M]_{f_{nl}=0}$, deviates appreciably from unity, much higher than the ratio of $[dN/d\ln M]_{f_{nl}=250}$ to $[dN/d\ln M]_{f_{nl}=0}$. Thus, the EZL mass function of the low-mass isolated clusters may be useful only for putting an upper limit on the value f_{nl}.

4. CONCLUSION AND DISCUSSION

We have incorporated primordial non-Gaussianity of the local type into the EZL formula for the halo mass function which was originally developed by Lim & Lee (2013) for the case of Gaussian initial conditions. Testing the EZL formula for two different cases of the primordial non-Gaussianity parameter ($f_{nl} = 60,\ 250$) as well as for the Gaussian case ($f_{nl} = 0$) at three different redshifts ($z = 0,\ 0.67,\ 1$) against the numerical results from high-resolution N-body simulations, we have found that the EZL mass functions agree excellently with the numerical results for every case considered and that its three model parameters have constant best-values, being independent of z and f_{nl}.

We have also constructed the EZL mass function of the isolated clusters which turns out to have only one model parameter other than the overall normalization factor. The constant value of the single parameter has been found to yield remarkable agreements with the N-body results for all of the three cases of f_{nl} at all of the three redshifts. Then, we have shown that although the abundance of the isolated clusters evaluated by the EZL formula is much more sensitive to the change of the value of f_{nl} than that of all clusters in the high-mass end, the practical usefulness of the EZL mass function of the isolated clusters is limited to putting an upper limit on the value of f_{nl} due to the relatively large Poisson errors.

In the current work, we have restricted our investigation to the case of primordial non-Gaussianity of the local type because the joint probability density of the linear shear eigenvalues, Equations (4)-(11), which are the key quantities in the EZL framework, are valid only for the case of local primordial non-Gaussianity. Furthermore, our formula is also limited to the case that f_{nl} is not large since Equation (4) is the first order approximation. To use the EZL mass function of the clusters as a probe of primordial non-Gaussianity, however, it will be desirable to derive the higher order approximation of the probability density distribution of the shear eigenvalues and to find its expression also for the other types of primordial non-Gaussianity.

A more fundamental issue about the EZL mass function is to find a physical meaning of its characteristic model parameters. As stated explicitly in Lim & Lee (2013), the EZL mass function is a mere phenomenological fitting formula and thus its characteristic parameters have nothing to do with a collapse condition. In other words, the best-fit values of the EZL parameters contain no information on the underlying dynamics that governs real process of the gravitational collapse of the density inhomogeneities . A remaining crucial question is why and how the EZL parameters stay constant against the changes of redshifts, the key cosmological parameters, and even the primordial non- Gaussianity parameter in spite of the fact that they are just fitting parameters. We plan to work on the above two issues and report the result elsewhere in the future.

We are very grateful to C.Wagner for kindly making his simulation data available to us. We also thank T.Y.Lam for helpful discussion. JL was supported by Basic Science Research Program through the National Research Foundation of Korea(NRF) funded by the Ministry of Education (NO. 2013004372) and partially by the research grant from the National Research Foundation of Korea to the Center for Galaxy Evolution Research (NO. 2010-0027910).

REFERENCES

Achitouv, I. E., & Corasaniti, P. S. 2012, JCAP, 7, E01

Achitouv, I., Rasera, Y., Sheth, R. K., & Corasaniti, P. S. 2013, Physical Review Letters, 111, 231303

Achitouv, I., Wagner, C., Weller, J., & Rasera, Y. 2013, arXiv:1312.1364

Audit, E., Teyssier, R., & Alimi, J. M. 1997, A&A, 325, 439

Babich, D., Creminelli, P., & Zaldarriaga, M. 2004, JCAP, 8, 9

Bartolo, N., Komatsu, E., Matarrese, S., & Riotto, A. 2004, Phys. Rep., 402, 103

Benson, A. J., Reichardt, C., & Kamionkowski, M. 2002, MNRAS, 331, 71

Bernardeau, F. 1994, ApJ, 427, 51

Bond, J. R., Cole, S., Efstathiou, G., & Kaiser, N. 1991, ApJ, 379, 440

Bond, J. R., & Myers, S. T. 1996, ApJS, 103, 1

Bond, J. R., & Myers, S. T. 1996, ApJS, 103, 41

Chiueh, T., & Lee, J. 2001, ApJ, 555, 83

Corasaniti, P. S., & Achitouv, I. 2011a, Physical Review Letters, 106, 241302

Corasaniti, P. S., & Achitouv, I. 2011b, Phys. Rev. D, 84, 023009

Courtin, J., Rasera, Y., Alimi, J.-M., et al. 2011, MNRAS, 410, 1911

Crocce, M., Fosalba, P., Castander, F. J., & Gaztañaga, E. 2010, MNRAS, 403, 1353

Dalal, N., Doré, O., Huterer, D., & Shirokov, A. 2008, Phys. Rev. D, 77, 123514

de Simone, A., Maggiore, M., & Riotto, A. 2011, MNRAS, 412, 2587

Desjacques, V. 2008, MNRAS, 388, 638

Desjacques, V., & Smith, R. E. 2008, Phys. Rev. D, 78, 023527

Despali, G., Tormen, G., & Sheth, R. K. 2013, MNRAS, 431, 1143

Doroshkevich, A. G. 1970, Astrofizika, 6, 581

Hamilton, J.-C. 2013, arXiv:1304.4446

Jedamzik, K. 1995, ApJ, 448, 1

Jenkins, A., et al. 2001, MNRAS, 321, 372

Knollmann, S. R., & Knebe, A. 2009, ApJS, 182, 608

Lam, T. Y., & Sheth, R. K. 2009, MNRAS, 395, 1743

Lam, T. Y., & Sheth, R. K. 2009, MNRAS, 398, 2143

Lam, T. Y., Sheth, R. K., & Desjacques, V. 2009, MNRAS, 399, 1482

Lee, J., & Shandarin, S. F. 1998, ApJ, 500, 14

Lee, J. 2012, ApJ, 752, 40

Lim, S., & Lee, J. 2013, JCAP, 1, 19

Lim, S., & Lee, J. 2014, ApJ, 783, 39

Lo Verde, M., Miller, A., Shandera, S., & Verde, L. 2008, JCAP, 4, 14

Lucchin, F., & Matarrese, S. 1988, ApJ, 330, 535

Maggiore, M., & Riotto, A. 2010, ApJ, 711, 907

Maggiore, M., & Riotto, A. 2010, ApJ, 717, 515

Maggiore, M., & Riotto, A. 2010, ApJ, 717, 526

Matarrese, S., Verde, L., & Jimenez, R. 2000, ApJ, 541, 10

Monaco, P. 1995, ApJ, 447, 23

Monaco, P. 1997, MNRAS, 287, 753

Monaco, P. 1997, MNRAS, 290, 439

Musso, M., & Sheth, R. K. 2012, MNRAS, 423, L102

Paranjape, A., & Sheth, R. K. 2012, MNRAS, 426, 2789

Paranjape, A., Lam, T. Y., & Sheth, R. K. 2012, MNRAS, 420, 1429

Paranjape, A., Sheth, R. K., & Desjacques, V. 2013, MNRAS, 431, 1503

Pillepich, A., Porciani, C., & Hahn, O. 2010, MNRAS, 402, 191

Planck Collaboration, Ade, P. A. R., Aghanim, N., et al. 2013, arXiv:1303.5076

Planck Collaboration, Ade, P. A. R., Aghanim, N., et al. 2013, arXiv:1303.5080

Planck Collaboration, Ade, P. A. R., Aghanim, N., et al. 2013, arXiv:1303.5084

Porciani, C., Dekel, A., & Hoffman, Y. 2002, MNRAS, 332, 339

Press, W. H., & Schechter, P. 1974, ApJ, 187, 425

Reed, D., Gardner, J., Quinn, T., Stadel, J., Fardal, M., Lake, G., & Governato, F. 2003, MNRAS, 346, 565

Riess, A. G., Macri, L., Casertano, S., et al. 2011, ApJ, 732, 129

Robertson, B. E., Kravtsov, A. V., Tinker, J., & Zentner, A. R. 2009, ApJ, 696, 636

Scoccimarro, R., Sefusatti, E., & Zaldarriaga, M. 2004, Phys. Rev. D, 69, 103513

Shen, J., Abel, T., Mo, H. J., & Sheth, R. K. 2006, ApJ, 645, 783

Sheth, R. K., & Tormen, G. 1999, MNRAS, 308, 119

Sheth, R. K., Mo, H. J., & Tormen, G. 2001, MNRAS, 323, 1

Sheth, R. K., & Tormen, G. 2002, MNRAS, 329, 61

Song, H., & Lee, J. 2009, ApJ, 701, L25

Springel, V. 2005, MNRAS, 364, 1105

Springel, V., Frenk, C. S., & White, S. D. M. 2006, Nature, 440, 1137

Tinker, J. L., et al. 2008, ApJ, 688, 709

Verde, L., Jimenez, R., Kamionkowski, M., & Matarrese, S. 2001, MNRAS, 325, 412

Wagner, C., Verde, L., & Boubekeur, L. 2010, JCAP, 10, 22

Wagner, C., & Verde, L. 2012, JCAP, 3, 2

Wang, L. & Steinhardt, P. J. 1998, ApJ, 508, 483

Warren, M. S., Abazajian, K., Holz, D. E., & Teodoro, L. 2006, ApJ, 646, 881

Yano, T., Nagashima, M., & Gouda, N. 1996, ApJ, 466, 1

Zentner, A. R. 2007, International Journal of Modern Physics D, 16, 763

This preprint was prepared with the AAS LaTeX macros v5.2.

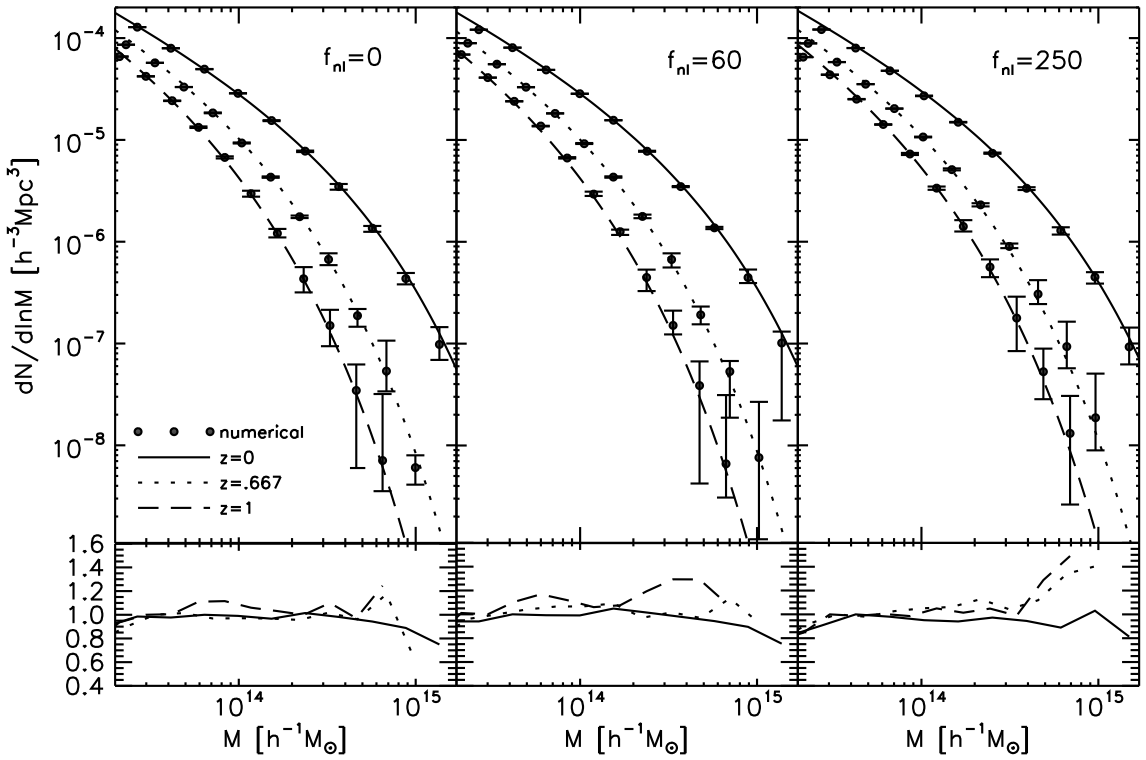

Fig. 1.— (Top panels): Number densities of the cluster-size halos as dots with Jackknife erros at three different redshifts for three different cases of primordial non-Gaussianity of the local type: $f_{nl} = 0,\ 60,\ 250$ in the left, middle and right panel, respectively. In each panel, the EZL mass function with the best-fit values of $\lambda_{1c} =$, $\lambda_{2c} =$, λ_{3c} are also plotted as solid ($z = 0$), dotted ($z = 0.66$) and dashed ($z = 1$) line, respectively. (Bottom panel): Ratios of the EZL mass functions to the corresponding numerical redshifts.

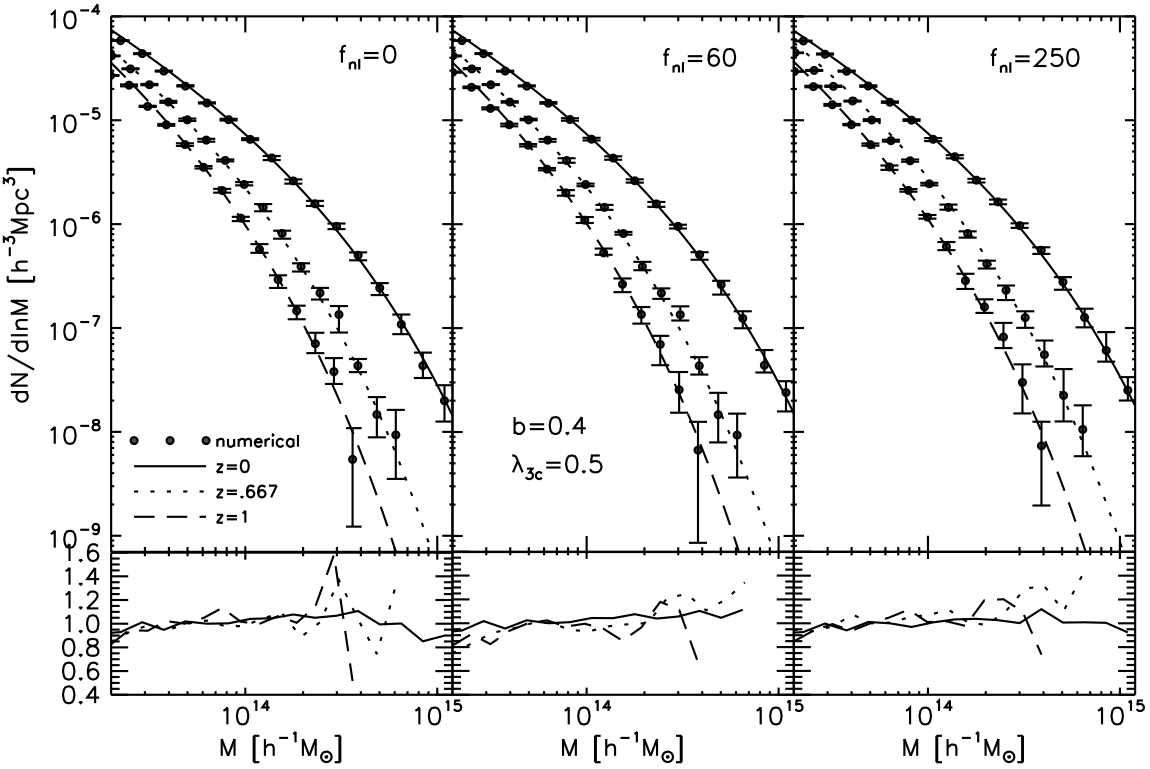

Fig. 2.— Same as Figure 1 but for the case of the isolated clusters.

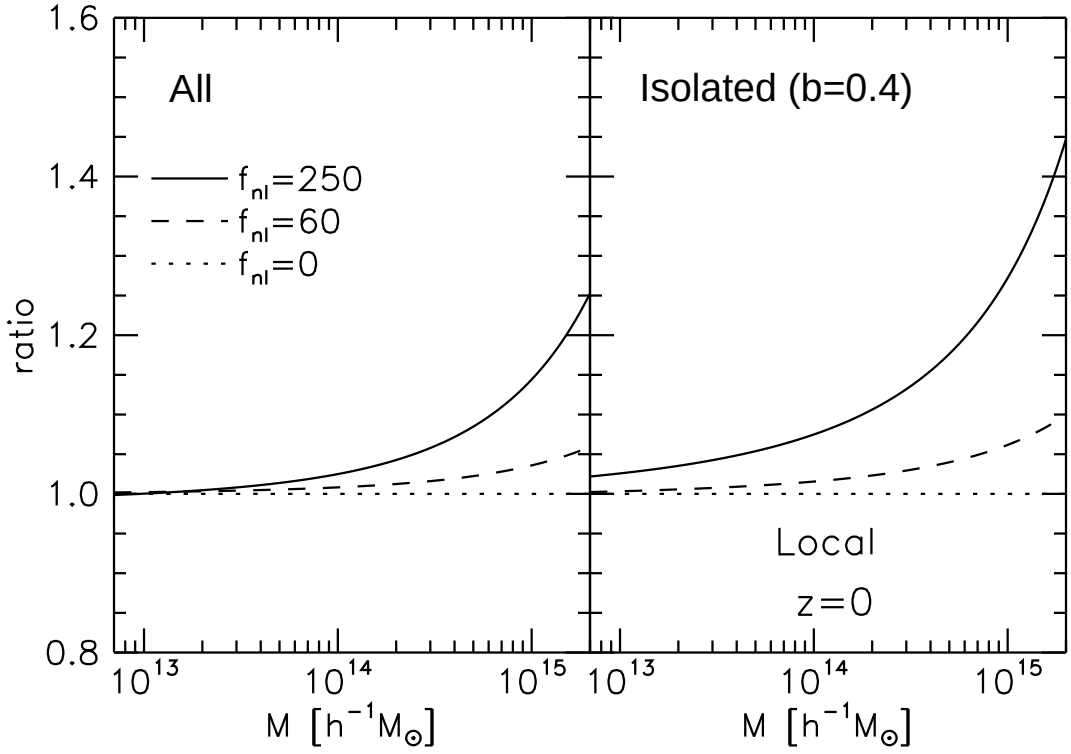

Fig. 3.— Ratios of the mass functions with primordial non-Gaussianity of the local type to the Gaussian ones at $z = 0$. The left and the right panels corresponds to the cases of all clusters and isolated clusters, respectively.

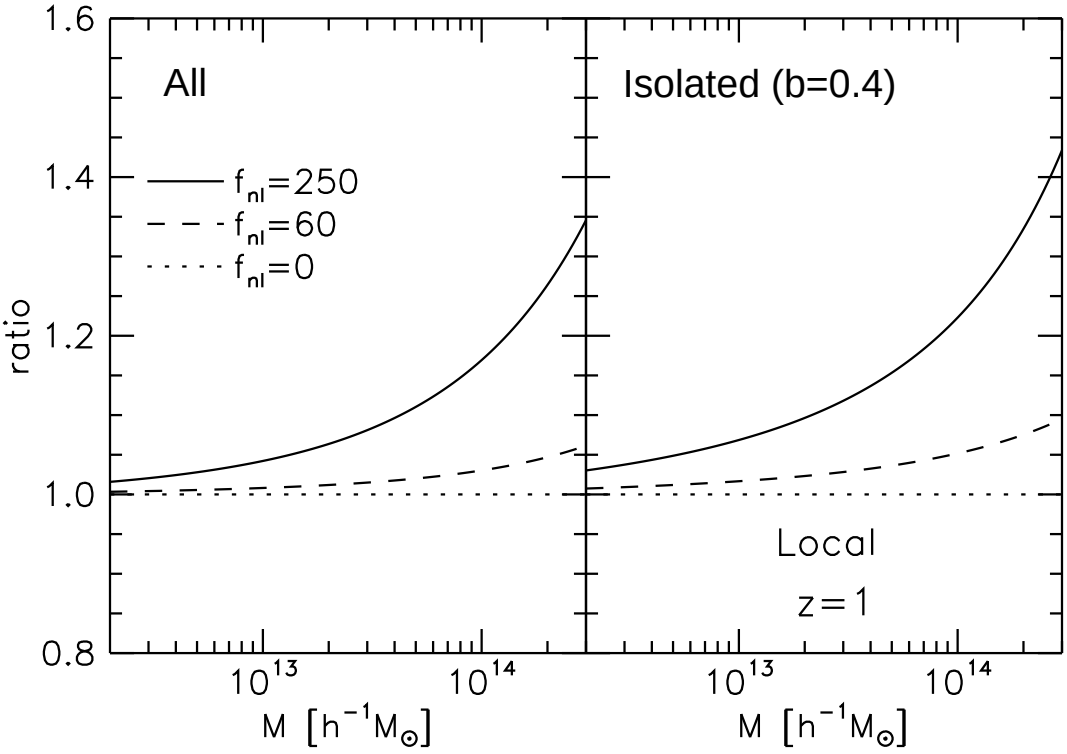

Fig. 4.— Same as Figure 3 but at $z = 1$.

Table 1. primordial non-Gaussianity parameter, total number and mean mass of the isolated clusters at $z = 0$.

f_{nl}	$N_{\rm I,tot}$	$\bar{M}$ $[10^{13}\,h^{-1}M_{\odot}]$
0	823903	2.75
60	824430	2.76
250	820363	2.78

Table 2. Same as Table 1 but at $z = 0.67$.

f_{nl}	$N_{\rm I,tot}$	$\bar{M}$ $[10^{13}\,h^{-1}M_{\odot}]$
0	508980	2.22
60	512175	2.22
250	516260	2.25

Table 3. Same as Table 1 but at $z = 1$.

f_{nl}	$N_{\rm I,tot}$	$\bar{M}$ $[10^{13}\,h^{-1}M_{\odot}]$
0	352303	1.98
60	356343	1.99
250	364036	2.02